


Extracellular signal-regulated kinase phosphorylation enhancement and Na_v1.7 sodium channel upregulation in rat dorsal root ganglia neurons contribute to resiniferatoxin-induced neuropathic pain: The efficacy and mechanism of pulsed radiofrequency therapy

Molecular Pain
Volume 18: 1–12
© The Author(s) 2022
Article reuse guidelines:
sagepub.com/journals-permissions
DOI: 10.1177/17448069221089784
journals.sagepub.com/home/mpi


Kotaro Hidaka¹, Toyoaki Maruta^{1*}, Tomohiro Koshida¹, Mio Kurogi¹, Yohko Kage², Satoshi Kouroki¹, Tetsuro Shirasaka¹, Ryu Takeya², and Isao Tsuneyoshi¹

Abstract

Pulsed radiofrequency (PRF) therapy is one of the most common treatment options for neuropathic pain, albeit the underlying mechanism has not been hitherto elucidated. In this study, we investigated the efficacy and mechanism of PRF therapy on resiniferatoxin (RTX)-induced mechanical allodynia, which has been used as a model of postherpetic neuralgia (PHN). Adult male rats were intraperitoneally injected with a vehicle or RTX. Furthermore, PRF current was applied on a unilateral sciatic nerve in all RTX-treated rats. On both ipsilateral and contralateral sides, the paw mechanical withdrawal thresholds were examined and L4-6 dorsal root ganglia (DRG) were harvested. In the DRG of rats with RTX-induced mechanical allodynia, Na_v1.7, a voltage-gated Na⁺ channel, was upregulated following the enhancement of extracellular signal-regulated kinase phosphorylation. Early PRF therapy, which was applied 1 week after RTX exposure, suppressed this Na_v1.7 upregulation and showed an anti-allodynic effect; however, late PRF therapy, which was applied after 5 weeks of RTX exposure, failed to inhibit allodynia. Interestingly, late PRF therapy became effective after daily tramadol administration for 7 days, starting from 2 weeks after RTX exposure. Both early PRF therapy and late PRF therapy combined with early tramadol treatment suppressed Na_v1.7 upregulation in the DRG of rats with RTX-induced mechanical allodynia. Therefore, Na_v1.7 upregulation in DRG is related to the development of RTX-induced neuropathic pain; moreover, PRF therapy may be effective in the clinical management of patients with PHN via Na_v1.7 upregulation inhibition.

Keywords

resiniferatoxin, postherpetic neuralgia, pulsed radiofrequency, ERK phosphorylation, Na_v1.7

Date Received: 16 November 2021; accepted: 7 March 2022

Introduction

Neuropathic pain is caused by peripheral or central nervous system damage or dysfunction.¹ The mechanism of neuropathic pain development varies depending on the cause (such as trauma and inflammation) as well as the degree and site of damage; thus, the complexity of the mechanism makes neuropathic pain difficult to treat. Neuropathic pain caused by

¹Faculty of Medicine, Department of Anesthesiology, University of Miyazaki, Miyazaki, Japan

²Faculty of Medicine, Department of Pharmacology, University of Miyazaki, Miyazaki, Japan

Corresponding Author:

Toyoaki Maruta, Faculty of Medicine, Department of Anesthesiology, University of Miyazaki, 5200 Kihara, Kiyotake, Miyazaki 889-1692, Japan.
Email: mmctm2@yahoo.co.jp



Creative Commons Non Commercial CC BY-NC: This article is distributed under the terms of the Creative Commons Attribution-NonCommercial 4.0 License (<https://creativecommons.org/licenses/by-nc/4.0/>) which permits non-commercial use, reproduction and distribution of the work without further permission provided the original work is attributed as specified on the SAGE

and Open Access pages (<https://us.sagepub.com/en-us/nam/open-access-at-sage>).

herpes zoster is called zoster-associated pain (ZAP).² Herpes zoster is caused by recurrent varicella-zoster virus (VZV) infection. VZV latently infects the cerebral and spinal ganglia even after the initial infection is cured, and develops as herpes zoster when cell-mediated immunity decreases due to aging or immunosuppressive conditions. Almost half of octogenarians reportedly experience herpes zoster, which has become a particularly important disease in developed countries with an aging population.³ ZAP is classified as (1) prodromal pain before the onset of eruption, (2) acute pain at the onset of eruption, and (3) chronic pain after eruption healing (postherpetic neuralgia [PHN]). (1) and (2) are presumed to be nociceptive pain associated with nerve destruction and inflammation due to virus reactivation. (3) is mainly neuropathic pain due to the loss of function of destroyed ganglia and peripheral neurons. Clinical guidelines for neuropathic pain pharmacotherapy by the Japan Society of Pain Clinicians (JSPC) recommend the use of tricyclic antidepressants, serotonin/noradrenaline reuptake inhibitors, and $\alpha_2\delta$ calcium channel ligands (gabapentinoids), such as amitriptyline, duloxetine, and pregabalin/gabapentin, respectively, prior to opioid use.⁴ Tramadol is a characteristic weak opioid that combines opioid receptor activity and serotonin/noradrenaline reuptake inhibition:⁵ both of these actions are synergistic in producing a relatively strong analgesic effect. Tramadol is considered a second-line treatment for neuropathic pain prior to the use of strong opioids and is reportedly effective against PHN.^{4,5} When these drug therapies are not sufficiently effective, nerve blocks, such as epidural and sympathetic nerve blocks, are used in combination with pharmacotherapy. However, although temporary relief can be obtained using these blocks, it is often difficult to achieve complete pain relief.

Pulsed radiofrequency (PRF) therapy has become a popular therapeutic modality for chronic pain in recent years because of its clinical efficacy and lack of tissue destructive effects.⁶ It is a technique wherein electromagnetic waves (20-ms pulses at a frequency of 500 kHz) are applied close to the dorsal root ganglia (DRG) or sensory nerve to increase the mean temperature of the tip of an electrode to a maximum of 42°C. This technique was introduced by Sluijter to dissociate the effect of electromagnetic waves from thermal destruction caused by conventional continuous radiofrequency.⁷ Although *in vivo* studies—using multiple animal models of neuropathic pain—and clinical trials have confirmed the efficacy of PRF treatment, the molecular and cellular biological mechanisms by which PRF works remain unclear.^{6,8–10}

Resiniferatoxin (RTX), an ultrapotent analog of capsaicin that irreversibly binds to transient receptor potential vanilloid 1 (TRPV1), has been used to study the action of nociceptive C-fiber afferents. RTX produces long-lasting paradoxical changes in thermal and mechanical sensitivities by the depletion of TRPV1-expressing unmyelinated afferent neurons and pathological nerve sprouting and reorganization into the

spinal lamina II via myelinated afferent fiber damage; it diminishes the thermal pain sensitivity but increases sensitivity to tactile stimulation, which mimics the unique clinical symptoms of PHN.¹¹ Therefore, animals with RTX-induced pain have been used as non-viral PHN models.^{10,12} Tanaka et al.¹⁰ reported that PRF treatment was more effective when applied in the early stage (1–3 weeks after RTX treatment) of mechanical allodynia in RTX-induced rat pain models; increasing the duration of PRF exposure from 2 to 6 min showed a significant anti-allodynic effect without motor impairment, albeit not in the late stage (5 weeks after RTX treatment).

This study aimed to investigate the mechanism by which PRF therapy causes RTX-induced mechanical allodynia recovery and the effects of early tramadol treatment on delayed PRF therapy in rats. In this investigation, we focused on the role of $\text{Na}_v1.7$, which is an important determinant of action potential thresholds in peripheral neurons, expressed in most nociceptive DRG and nerve endings in the epidermis and superficial membranes of the spinal cord dorsal horn.¹³ It was the first voltage-dependent Na^+ channel to be found with an altered functional mutation in humans.¹⁴ Gain-of-function mutations in *SCN9A*, which encodes $\text{Na}_v1.7$, lead to severe neuropathic pain, whereas loss-of-function mutations in this gene lead to an indifference to pain. $\text{Na}_v1.7$ supposedly enhance subthreshold stimuli, making it easy for neurons to reach the threshold for firing.¹⁵ $\text{Na}_v1.7$ acts as an amplifier of the receptor potential in nociceptive neurons; moreover, it plays a critical role in inherited erythromelalgia and paroxysmal extreme pain disorder, as it causes gain-of-function mutations that enable the channel to open with small depolarizations. Congenital insensitivity to pain is known as a loss-of-function mutation in $\text{Na}_v1.7$. Patients with a loss-of-function mutation in *Nav1.7* have no cognitive or cardiac function impairment; analgesic therapies targeting $\text{Na}_v1.7$ have been investigated using these *SCN9A* mutations. Although conventional global knockout of *SCN9A* in mice is neonatally lethal, loss-of-function *SCN9A* mutations can enable the development of global *SCN9A* knockout mice or rats that can survive.¹⁶ Animal studies have shown that $\text{Na}_v1.7$ expression and function are increased in models of diabetic neuropathy, chronic constrictive sciatic nerve injury, and chemotherapy-induced peripheral neuropathy.¹⁷ Specifically, a previous study demonstrated *Nav1.7* mRNA upregulation and sodium current density increase in ND7/23-*Nav1.8* neuroblastoma cells infected with PHN-associated VZV, which were abolished by tetrodotoxin exposure.¹⁸ Thus, we predicted that $\text{Na}_v1.7$ expression may be a key factor in the development of RTX-induced neuropathic pain.

Materials and methods

Animal ethics

This study was conducted in strict accordance with the guidelines for the Proper Conduct of Animal Experiments (Science Council of Japan). These experiments were

approved by the Experimental Animal Care and Use Committee of the University of Miyazaki (approval number: 2018-534). Efforts were made to minimize the number of animals used and their suffering.

Primary culture of rat DRG neurons and test drug application

Sprague-Dawley rats (aged 3 weeks, male, purchased from Kudo, Japan) were terminally anesthetized with sevoflurane, and DRG were dissected. The neurons were isolated for 3–4 days in Dulbecco's modified Eagle's medium supplemented with 10% fetal bovine serum at 37°C in a humidified atmosphere of 95% air and 5% CO₂. Thereafter, the neurons were treated in a fresh medium with 1 nM, 10 nM, 100 nM, and 1 μM RTX (LC Laboratories, Woburn, MA, USA) for 7 days. A medium-containing vehicle (a mixed solvent of 10% Tween 80, 10% ethanol, and saline) was used in rats that were assigned to the vehicle group. Na_v1.7 protein levels were measured using western blot analysis.

Animal characteristics and pharmacological treatments

Adult male Sprague-Dawley rats weighing approximately 250–400 g were used in this study. During the experiments, all rats were housed in a temperature- and humidity-controlled environment with a 12-h light-dark cycle and were given free access to food and water.

An RTX-induced neuropathic pain model was used. This model was reported by Pan et al., and is considered to have a pathologic mechanism that is more comparable to that of PHN than that induced using the nerve ligation method.^{10–12} RTX was dissolved in a mixed solvent of 10% Tween 80, 10% ethanol, and saline to obtain a 100-μg/mL concentration. RTX (250 μg/kg) was administered intraperitoneally (i.p.) to rats under anesthesia by 2–3% sevoflurane. Only a solvent vehicle was administered i.p. to rats in the vehicle group. Rats were transferred to their cages after the recovery period and were classified into groups as described below.

In the first series of *in vivo* experiments, we investigated the alterations of Na_v1.7 expression and extracellular signal-regulated kinase (ERK) phosphorylation in the DRG of rats with RTX-induced neuropathic pain. Vehicle (vehicle group) or RTX was injected i.p. Rats with RTX-induced neuropathic pain were subjected to PRF current in the right sciatic nerve for 2 min after 1 week of RTX administration (RTX + early PRF group), and the withdrawal thresholds of the ipsilateral and contralateral paws were examined using the von Frey test. PRF current was not applied to the left sciatic nerve (RTX group). Moreover, the von Frey test was performed before as well as 1, 2, 3, 4, and 5 weeks after RTX or vehicle treatment. On the second or fifth week after RTX or vehicle treatment, the rats were decapitated after inhalational

sevoflurane-induced loss of consciousness, and L4-L6 DRG were dissected from rats in each group; Na_v1.7 and ERK expressions were measured using reverse transcription polymerase chain reaction (RT-PCR) and/or western blot analysis.

In the second series of *in vivo* experiments, we investigated the long-term effects of RTX treatment and the efficacy of late PRF treatment following tramadol administration in rats with RTX-induced neuropathic pain. Vehicle (vehicle group), RTX or RTX + tramadol was injected i.p. Moreover, all rats with RTX-induced neuropathic pain received PRF current (as described above) 5 weeks after RTX treatment, and the withdrawal thresholds of the ipsilateral (RTX + late PRF group) and contralateral (RTX group) paws were examined. Tramadol (Sigma-Aldrich, St Louis, MO, USA) was dissolved in sterile saline to obtain a solution with a concentration of 20-mg/mL. Tramadol (20 mg/kg) was administered i.p. once daily for 7 days, starting 2 weeks after RTX administration. PRF treatment was administered (as described above) 5 weeks after RTX treatment (2 weeks after the end of tramadol administration), and the withdrawal thresholds of the ipsilateral (RTX + Tramadol + late PRF group) and contralateral paws (RTX + Tramadol group) were examined. The von Frey test was performed before and every week after RTX or vehicle administration. On the ninth week after RTX or vehicle treatment, L4-L6 DRG were dissected from rats in each group as described above, and Na_v1.7 expression was measured using RT-PCR and western blot analysis.

PRF procedures

Rats were anesthetized with medetomidine (0.375 mg/kg; ZENOAQ, Koriyama, Japan), buprenorphine (2.5 mg/kg; Meiji Seika, Tokyo, Japan), and midazolam (2 mg/kg; SANDOZ, Tokyo, Japan); PRF was applied with the rats in the prone position. All RTX-treated rats received PRF treatment on the right sciatic nerve. A 54-mm, 22-gauge guiding needle with a 4-mm active tip (Ac-4; Hakko, Tokyo, Japan) was introduced percutaneously at an anatomically defined region known as the sciatic notch (located between the greater trochanter and ischial tuberosity). After the puncture, the stylet of the needle was replaced with a radiofrequency probe, tissue impedance was measured, and the presence of muscle contractions was checked using a 3-Hz electrical stimulation to a maximum output of 1.0 V. If muscle contractions were observed with an output lower than 0.5 V, the electrode was pulled back by 1 mm. If muscle contractions were observed with an output higher than 1.0 V or no contraction was observed, the electrode was advanced by 1 mm. The procedure was repeated until muscle contractions were observed with an appropriate output ranging between 0.5 and 1.0 V. This criterion indicated that the electrode was near the sciatic nerve but did not penetrate it. After proper electrode placement, the PRF procedure was performed for 2 min, using a

radiofrequency generator with standard clinical specifications (model JK3; RDG Medical, Surrey, UK). The PRF current was applied in 20-ms pulses every 500 ms (20 ms of 500-kHz RF pulses, delivered at a frequency of 2 Hz). The maximum temperature was automatically maintained at 42°C. The mean impedance values of PRF current were $534.4 \pm 50.2 \Omega$, $603.3 \pm 83.1 \Omega$, and $560.0 \pm 53.5 \Omega$ in the RTX + early PRF, RTX + late PRF, and RTX + Tramadol + late PRF groups, respectively; there were no significant differences among these three groups.

Von Frey test

Mechanical sensitivity was examined by testing the paw withdrawal threshold using an electronic von Frey anesthesiometer (IITC Life Science Inc., Woodland Hills, CA, USA). Briefly, each rat was placed in a 20 cm × 20 cm suspended chamber on a metallic mesh floor. After an acclimation period of 30 min, a polypropylene tip was applied perpendicularly to the tip of the plantar surface of the right and left hind paws for 3–4 s. Brisk withdrawal or paw flinching was considered a positive response, and the mean of three measurements was considered the pain threshold.

Western blot analysis

In the *in vitro* study, 7 days after RTX or vehicle treatment, the cultured DRG neurons were harvested and homogenized in an ice-cold lysis buffer composed of 1% Triton X-100, 150 mM NaCl, 1 mM EDTA, and 20 mM Tris-HCl, pH 7.5, with added protease and phosphatase inhibitor cocktails (Roche Diagnostics, Mannheim, Germany); the mixture was centrifuged at 12,000 r/min and 4°C for 10 min. The supernatant was collected and stored at –80°C until use. The total protein content was determined in each sample using the Bradford method-based protein assay kit (Aproscience, Naruto, Japan) with bovine serum albumin (BSA) as a protein standard. The stored supernatants were solubilized in a 2×SDS electrophoresis sample buffer and heated at 98°C for 5 min. Equal amounts of proteins (7.0–7.5 µg per lane) were separated by SDS-12% polyacrylamide gel electrophoresis and transferred onto a polyvinylidene difluoride membrane (Immobilon-P, Merck Millipore, Burlington, MA, USA). The membrane was subsequently incubated with a blocking solution (2% BSA in Tween-Tris-buffered saline [10 mM Tris-HCl, pH 7.4, 150 mM NaCl, and 0.1% Tween-20]) and further incubated overnight at 4°C in 2% BSA with rabbit anti-Na_v1.7 polyclonal antibody (1:1000, ASC-008, Alomone Labs, Jerusalem, Israel) or Can Get Signal Solution-1 (TOYOBO, Osaka, Japan) with mouse anti-β-actin monoclonal antibody (1:5000, A5441, Sigma-Aldrich, St Louis, MO, USA).

In the *in vivo* study, the collected L4-L6 DRG tissues from each rat were mechanically homogenized in ice-cold lysis buffer, and proteins were extracted in the same manner as mentioned above. The membrane was incubated overnight at

4°C in 2% BSA with rabbit anti-Na_v1.7 polyclonal antibody, Can Get Signal Solution-1 with rabbit anti-ERK polyclonal antibody (1:2000, K-23, Santa Cruz, Dallas, TX, USA), mouse anti-p-ERK monoclonal antibody (1:2000, E-4, Santa Cruz), or mouse anti-β-actin monoclonal antibody (1:5000, A5441, Sigma-Aldrich, St Louis, MO, USA).

In both *in vitro* and *in vivo* studies, after incubation with each primary antibody, the process proceeded to incubation with each secondary antibody. After repeated washing, the immunoreactive bands were developed using Can Get Signal Solution-2 with horseradish peroxidase-conjugated anti-rabbit antibody (1:5000, GE Healthcare Japan Corporation, Tokyo, Japan) or anti-mouse antibody (1:5000, Santa Cruz), visualized using an enhanced ImmunoStar LD (Fuji Film, Tokyo, Japan), and captured in a LAS-4000 luminoimage analyzer (Fuji Film, Tokyo, Japan). The commercially available molecular weight markers Amersham ECL rainbow marker-full range (GE Healthcare Japan Corporation, Tokyo, Japan) and Precision Plus Protein Kaleidoscope Standards (Bio-Rad Laboratories Inc., Hercules, CA, USA), consisting of proteins of molecular weight 12–225 kDa and 10–250 kDa, respectively, were used as molecular weight references (Supplementary Figure 1). The densities of protein blots were quantified using ImageJ,¹⁹ and the protein levels were normalized to β-actin levels.

RT-PCR

The dissected DRG tissues were homogenized, and total cellular RNA was isolated from cells by acid guanidine thiocyanate-phenol-chloroform extraction using TRIzol reagent (Total RNA Isolation Reagent, Invitrogen, Waltham, Massachusetts, USA). The quality and quantity of total RNA were assessed using the ratio of optical densities at 260 and 280 nm. The reverse transcription reaction was performed using a first-strand cDNA synthesis kit (SuperScript II Reverse Transcriptase, Invitrogen, Waltham, Massachusetts, USA), according to the manufacturer's protocol. PCR amplification was performed using GoTaq Green Master Mix (Promega, Madison, WI, USA), 1 µL of cDNA template, as well as forward and reverse primers (each at 4 µM), in a 25-µL solution. The target cDNA was amplified using a PCR protocol consisting of the initial denaturation step (10 min at 95°C), followed by 27 cycles of the denaturation step, the annealing step, the extension step (10 s at 98°C, 30 s at 55°C, and 60 s at 72°C for β-actin; 10 s at 98°C, 30 s at 58°C, and 60 s at 72°C for Na_v1.7), and the final extension step (90 s at 72°C). PCR was performed in a thermal cycler (Veriti® Thermal Cycler, Thermo Fisher Scientific, Waltham, MA, USA). The PCR products were run on a 2% agarose gel and captured using a LAS-4000 luminoimage analyzer. We used the following specific primers that were obtained from Macrogen Global Headquarters (Seoul, South Korea): Na_v1.7-Forward, 5'-cgatgggtcaccgatttctctac-3'; Na_v1.7-

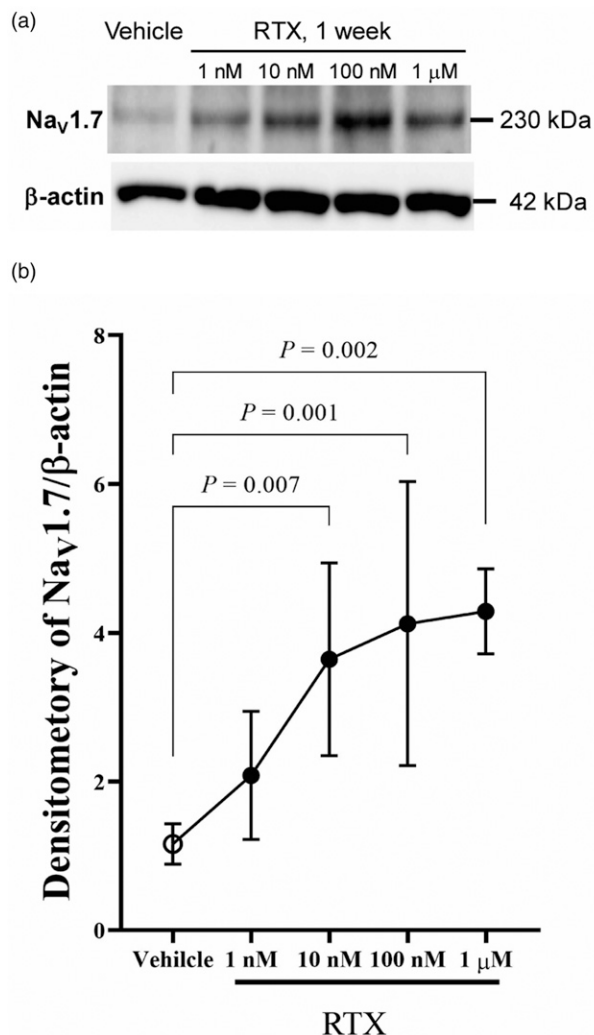


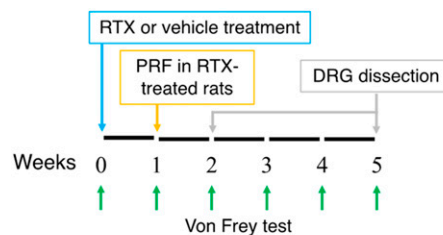
Figure 1. Upregulation of Nav1.7 expression by RTX in cultured rat DRG neurons. Cells were treated without or with RTX (1 nM–1 μM) for 1 week in a culture medium. The cell lysates were subjected to western blot analysis using antibodies against Nav1.7. (A) Representative western blot showing the RTX concentration-dependent upregulation of Nav1.7. Blots shown are typically obtained from five independent experiments with similar results. (B) A quantitative densitometric analysis of Nav1.7 expression ratio. Immunoreactivities were quantified using an immunoblot analyzer. Nav1.7 levels were normalized to β-actin levels at each incubation time. Data of five experiments are expressed as mean ± standard deviation. DRG, dorsal root ganglia; RTX, resiniferatoxin.

Reverse, 5'-cgtgaagaatgagccgaagat-3'; β-actin-Forward, 5'-cgttgacatccgtaagacctc-3'; and β-actin-Reverse, 5'-taggagcaggcagtaatct-3'.²⁰

Statistical analysis

Western blot and RT-PCR data were analyzed using one-way analysis of variance (ANOVA), followed by a post hoc Tukey

(a) The first series of in vivo experiments



(b) The second series of in vivo experiments

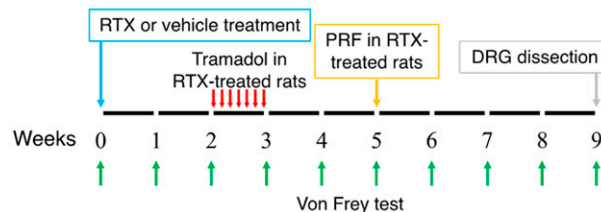


Figure 2. In vivo experimental design. (A) The first series of in vivo experiments. Vehicle or RTX was injected i.p., and the withdrawal thresholds were examined using the von Frey test before and every week after vehicle or RTX treatment until 2 or 5 weeks. In rats with RTX-induced neuropathic pain, PRF current was applied to the right sciatic nerve 1 week after RTX administration. The DRG were dissected 2 or 5 weeks after RTX administration. (B) The second series of in vivo experiments. Vehicle or RTX was injected i.p., and the withdrawal thresholds were examined using the von Frey test before and every week after vehicle or RTX treatment until 9 weeks. In rats with RTX-induced neuropathic pain, 2 weeks after RTX administration, tramadol was administered daily i.p. for 1 week, and PRF current was applied to the right sciatic nerve 5 weeks after RTX administration. DRG were dissected 9 weeks after RTX administration. RTX, resiniferatoxin; PRF, pulsed radiofrequency; DRG, dorsal root ganglia; i.p., intraperitoneally.

test. Behavioral tests were conducted on six rats in each group. Repeated measures of behavioral data were analyzed using two-way ANOVA, followed by the Tukey test. We compared the ipsilateral and contralateral paw withdrawal thresholds. Data are expressed as mean ± standard deviation for western blot and RT-PCR or mean ± standard error of the mean for the von Frey test. A value of $p < 0.05$ was considered statistically significant. Statistical analyses were performed using Prism 8 (GraphPad Software, San Diego, CA, USA) software for Windows.

Results

RTX-induced upregulation of Nav1.7 expression in cultured rat DRG neurons

Before the *in vivo* study, we used primary cultured DRG neurons to screen for which Na⁺ channel expression was altered by RTX, as previous studies have demonstrated that voltage-dependent Na⁺ channels, such as Nav1.7, Nav1.8,

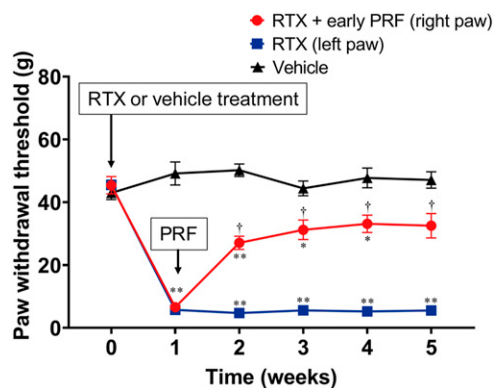


Figure 3. Paw withdrawal test (von Frey test) for RTX-induced mechanical allodynia and its treatment using early PRF therapy. RTX (200 $\mu\text{g}/\text{kg}$) or vehicle (a mixed solvent of 10% Tween 80, 10% ethanol, and saline) was administered i.p. RTX-treated rats received right sciatic nerve PRF therapy 1 week after RTX treatment. Mechanical allodynia was evaluated via the von Frey test, using an electrical von Frey meter. The von Frey test was performed before and 1 week after RTX or vehicle treatment. Paw withdrawal thresholds are shown for rats that were assigned to the vehicle, RTX (left paw), and RTX + early PRF (right paw) groups. This experimental design is shown in Figure 2(A). Data of six rats are expressed as mean \pm standard error of the mean. * $p < 0.01$ and ** $p < 0.001$, compared with vehicle treatment at each time point; † $p < 0.001$, compared with RTX treatment at each time point. RTX, resiniferatoxin; PRF, pulsed radiofrequency; i.p., intraperitoneally.

and $\text{Nav}_1.9$ expressed in DRG, are involved in neuropathic pain.^{14,21} Figure 1 shows an RTX-induced dose-dependent upregulation of $\text{Nav}_1.7$ protein expression in cultured DRG neurons.

Mechanical allodynia in a rat model of RTX-induced neuropathic pain

Figure 2(A) shows the protocol of the first series of *in vivo* experiments. Rats injected with RTX exhibited immediate behavioral reactions, including hyperexcitability and restlessness. However, these reactions were transient and gradually subsided within 1–3 h. Paw withdrawal thresholds of both hind paws 1 week after RTX treatment were significantly lower than those of rats that were administered the vehicle (Figure 3). PRF therapy resulted in mechanical allodynia recovery in the right paw.

Upregulation of $\text{Nav}_1.7$ expression following the enhancement of ERK phosphorylation in DRG neurons of rats with RTX-induced neuropathic pain

Using RT-PCR (Figures 4(A) and 4(B)) and western blot (Figures 4(C) and 4(D)) analyses, we demonstrated that RTX use induced an increase in $\text{Nav}_1.7$ expression, which was inhibited by early PRF therapy applied 1 week after RTX treatment.

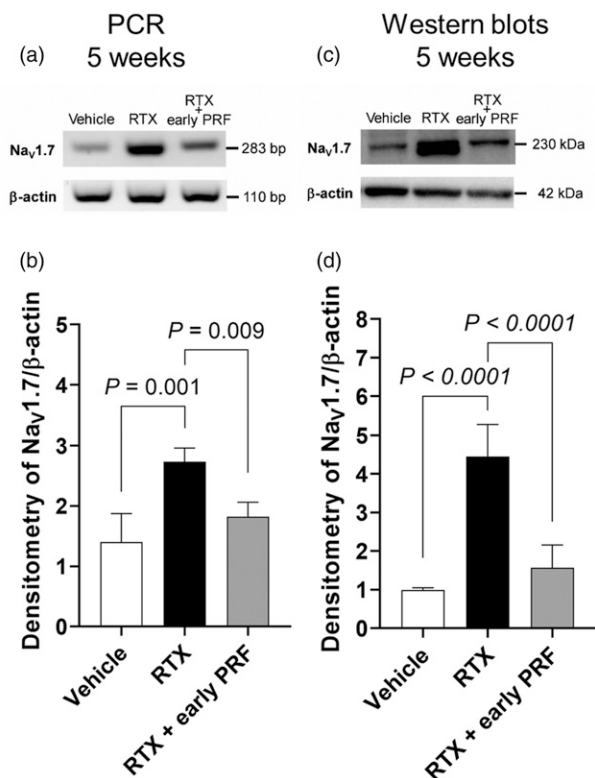


Figure 4. Inhibition of RTX-induced $\text{Nav}_1.7$ expression upregulation using early PRF treatment in rat DRG, 5 weeks after RTX treatment. RT-PCR (A) and representative western blot (C) showing that the mRNA and protein levels of $\text{Nav}_1.7$ were upregulated by RTX; this $\text{Nav}_1.7$ upregulation was inhibited by PRF treatment. Samples were harvested 5 weeks after RTX or vehicle treatment (4 weeks after PRF in the RTX + early PRF group). This experimental design is shown in Fig. 2A. Quantitative densitometric analyses of $\text{Nav}_1.7$ expression ratio for RT-PCR (B) and western blot (D). Data are expressed as mean \pm standard deviation, $n = 6$ samples (one animal per sample). RTX, resiniferatoxin; PRF, pulsed radiofrequency; RT-PCR, reverse transcription polymerase chain reaction; DRG, dorsal root ganglia.

The modulation of mitogen-activated protein kinase (MAPK) activation, including ERK, p38, and c-Jun N-terminal kinase (JNK) pathways, has been linked to the development of pain.^{22,23} Figure 5 illustrates RT-PCR and western blot analyses of ERK in the DRG of RTX-treated rats with or without PRF therapy compared to those of vehicle-treated rats. Although no difference was observed in the total ERK1/2 protein levels among the RTX, RTX + early PRF, and vehicle groups, phosphorylated ERK1/2 (p-ERK1/2) levels in the RTX group increased significantly up to 1.5-fold compared to those in the vehicle group, 2 weeks after RTX or vehicle treatment. This increase in p-ERK1/2 levels was abolished in the RTX + early PRF group (Figures 5(A) and 5(B)). In contrast, 5 weeks after RTX or vehicle treatment, there was no difference in p-ERK1/2 levels among the RTX + early PRF, RTX, and vehicle groups (Figures 5(C) and 5(D)).

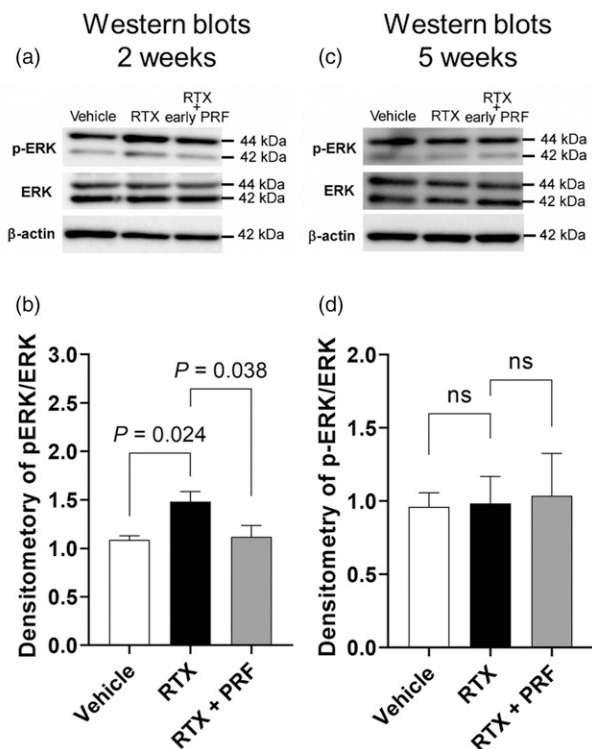


Figure 5. Temporal changes in the effects of RTX treatment and PRF therapy on ERK phosphorylation in rat DRG, 2 and 5 weeks after RTX treatment. (A) Representative western blot showing that the p-ERK/ERK expression ratio 2 weeks after RTX treatment was enhanced by RTX administration, and this enhancement was inhibited by PRF treatment. Samples were harvested 2 weeks after RTX or vehicle treatment (1 week after PRF therapy in the RTX + early PRF group). This experimental design is shown in Figure 2(A). (B) A quantitative densitometric analysis of p-ERK/ERK expression ratio. (C) Representative western blot showing the p-ERK/ERK expression ratio 5 weeks after RTX treatment. There was no difference in the p-ERK/ERK expression ratio among the groups. Samples were harvested 5 weeks after RTX or vehicle treatment (4 weeks after PRF therapy in the RTX + early PRF group). This experimental design is shown in Figure 2(A). (D) A quantitative densitometric analysis of p-ERK/ERK expression ratio. Data are expressed as mean \pm standard deviation, $n = 6$ samples (one animal per sample). RTX, resiniferatoxin; PRF, pulsed radiofrequency; DRG, dorsal root ganglia; ERK, extracellular signal-regulated kinase.

Effects of early tramadol treatment on late PRF therapy for RTX-induced neuropathic pain

Figure 6 shows the long-term course (up to 9 weeks after RTX treatment) of rats with RTX-induced mechanical allodynia. Late PRF therapy (5 weeks after RTX treatment) did not trigger RTX-induced mechanical allodynia recovery. However, as shown in Figure 7, when early tramadol treatment (2 weeks after RTX treatment) was administered, late PRF therapy (5 weeks after RTX treatment) triggered RTX-induced mechanical allodynia recovery. Early tramadol

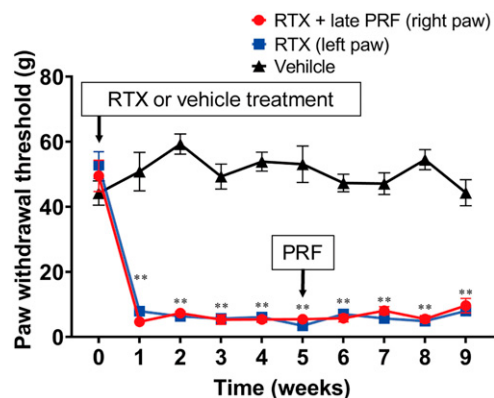


Figure 6. Long-term course of the paw withdrawal test with no inhibitory effects of late PRF therapy on RTX-induced mechanical allodynia. RTX (200 μ g/kg) or vehicle (a mixed solvent of 10% Tween 80, 10% ethanol, and saline) was administered i.p. RTX-treated rats received right sciatic nerve PRF therapy 5 weeks after RTX treatment. The von Frey test was performed before and 1 week after RTX or vehicle treatment. Paw withdrawal thresholds are shown for rats that were assigned to the vehicle, RTX (left paw), and RTX + late PRF (right paw) groups. Data are expressed as mean \pm standard deviation, $n = 6$ samples (one animal per sample). ** $p < 0.001$, compared with vehicle at each time. RTX, resiniferatoxin; PRF, pulsed radiofrequency; i.p., intraperitoneally.

treatment alone temporarily inhibited RTX-induced mechanical allodynia. Figure 2(B) shows the protocol of the second series of in vivo experiments. As shown by RT-PCR (Figures 8(A) and (B)) and western blot (Figures 8(C) and (D)) analyses, RTX continued to upregulate $Na_v1.7$ expression up to 9 weeks after RTX treatment, and late PRF therapy (5 weeks after RTX treatment) with early tramadol therapy suppressed the RTX-induced upregulation of $Na_v1.7$.

Discussion

We demonstrated that RTX use increased $Na_v1.7$ expression in a concentration-dependent manner in cultured DRG neurons. This suggested that RTX may act directly on the DRG to trigger $Na_v1.7$ upregulation that may be involved in the development of RTX-induced neuropathic pain. Furthermore, the next series of in vivo experiments demonstrated that $Na_v1.7$ expression upregulation following the enhancement of ERK phosphorylation in rat DRG neurons was strongly associated with the development of RTX-induced mechanical allodynia. Early PRF therapy can cause RTX-induced mechanical allodynia recovery by suppressing the abovementioned $Na_v1.7$ upregulation, whereas delayed PRF therapy cannot. However, by performing early tramadol treatment interposition, late PRF therapy can effectively trigger RTX-induced mechanical allodynia recovery by suppressing $Na_v1.7$ upregulation, akin to early PRF therapy.

PRF therapy can trigger RTX-induced mechanical allodynia recovery by inhibiting both ERK phosphorylation and

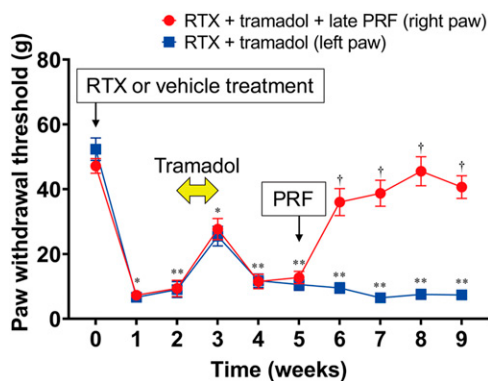


Figure 7. Long-term course of the paw withdrawal test for RTX-induced mechanical allodynia and the effect of early tramadol treatment on late PRF therapy. RTX (200 μ g/kg) was administered i.p. RTX-treated rats were injected with tramadol (20 mg/kg) i.p. daily for 7 days from 2 weeks after RTX treatment, and received right sciatic nerve PRF therapy 5 weeks after RTX treatment. The von Frey test was performed before and 1 week after RTX or vehicle treatment. Paw withdrawal thresholds are shown for rats that were assigned to the RTX + Tramadol (left paw) and RTX + Tramadol + late PRF (right paw) groups. This experimental design is shown in Figure 2(B). Data are expressed as mean \pm standard deviation, $n = 6$ samples (one animal per sample). * $p < 0.01$ and ** $p < 0.01$, compared with vehicle treatment in Figure 6 at each time point; † $p < 0.001$, compared with RTX treatment at each time. RTX, resiniferatoxin; PRF, pulsed radiofrequency; DRG, dorsal root ganglia; i.p., intraperitoneally.

$\text{Na}_V1.7$ upregulation. Yeh et al.²⁴ reported that ERK phosphorylation was increased in the spinal dorsal horns of spared nerve injury (SNI) model rats, and PRF application in the DRG elicited an anti-allodynic effect by ERK phosphorylation inhibition in dorsal horns. Although this report did not refer to Na^+ channels, the inhibition of $\text{Na}_V1.7$ expression may have been involved in the efficacy of PRF because $\text{Na}_V1.7$ expression in DRG was upregulated after SNI in another report.²⁵ Dai et al.²⁶ demonstrated that PRF application to the DRG in SNI model rats produces an analgesic effect and $\text{Na}_V1.7$ downregulation in the DRG. Both $\text{Na}_V1.7$ and MAPKs, including ERK, p38, and JNK pathways, play a vital role in the development of neuropathic pain. ERK—in the DRG and dorsal horn—is reportedly a major target molecule for neuropathic pain treatment. In addition to RTX, previous reports highlight that a plantar injection of capsaicin, an agonist of TRPV1, enhances ERK phosphorylation in rat DRG, causing transient thermal hyperalgesia.^{27,28} ERK activation suppression may be a promising therapeutic target for neuropathic pain treatment.²⁹ ERK and $\text{Na}_V1.7$ influence each other, as phosphorylated ERK1 lowers the activation threshold, making it easy to open the $\text{Na}_V1.7$ channel in response to weak stimuli.³⁰ We previously reported that ERK inhibitors impede veratridine-induced $^{22}\text{Na}^+$ influx, indicating that the basal constitutive activities of ERK may prime

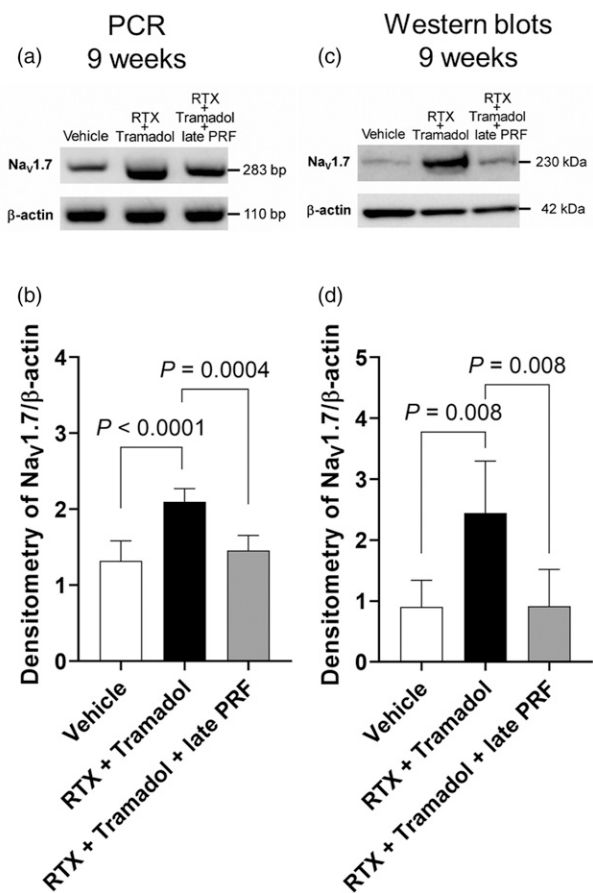


Figure 8. Inhibition of RTX-induced $\text{Na}_V1.7$ expression upregulation by early tramadol treatment with late PRF therapy in rat DRG. RT-PCR (A) and representative western blot (C) showing that protein and mRNA $\text{Na}_V1.7$ levels were upregulated by RTX treatment; $\text{Na}_V1.7$ upregulation was inhibited by late PRF therapy with early tramadol administration. Samples were harvested at 9 weeks after RTX or vehicle treatment (4 weeks after PRF in the RTX + Tramadol + late PRF group). This experimental design is shown in Figure 2(B). Quantitative densitometric analyses of the $\text{Na}_V1.7$ expression ratio for RT-PCR (B) and western blot (D). Data of six rats are expressed as mean \pm SD. RTX, resiniferatoxin; PRF, pulsed radiofrequency; DRG, dorsal root ganglia; RT-PCR, reverse transcription polymerase chain reaction.

$\text{Na}_V1.7$ channels to open.³¹ Furthermore, some neuropathic pain types, such as paclitaxel-induced peripheral neuropathy³² and pulpitis inflammatory pain,³³ resulted from the upregulation or gain-of-function of $\text{Na}_V1.7$ through ERK1/2 signaling.

PRF is used to achieve analgesia via pulsed irradiation with electromagnetic waves.⁶ The mechanisms of action of PRF are not well understood: it is thought to exert a neuromodulatory action that inhibits the expression of sensory neuron-specific molecules and genes involved in the development of neuropathic pain in the spinal dorsal horn and DRG.^{34–36} Yeh et al.²⁴ reported that the analgesic effect of

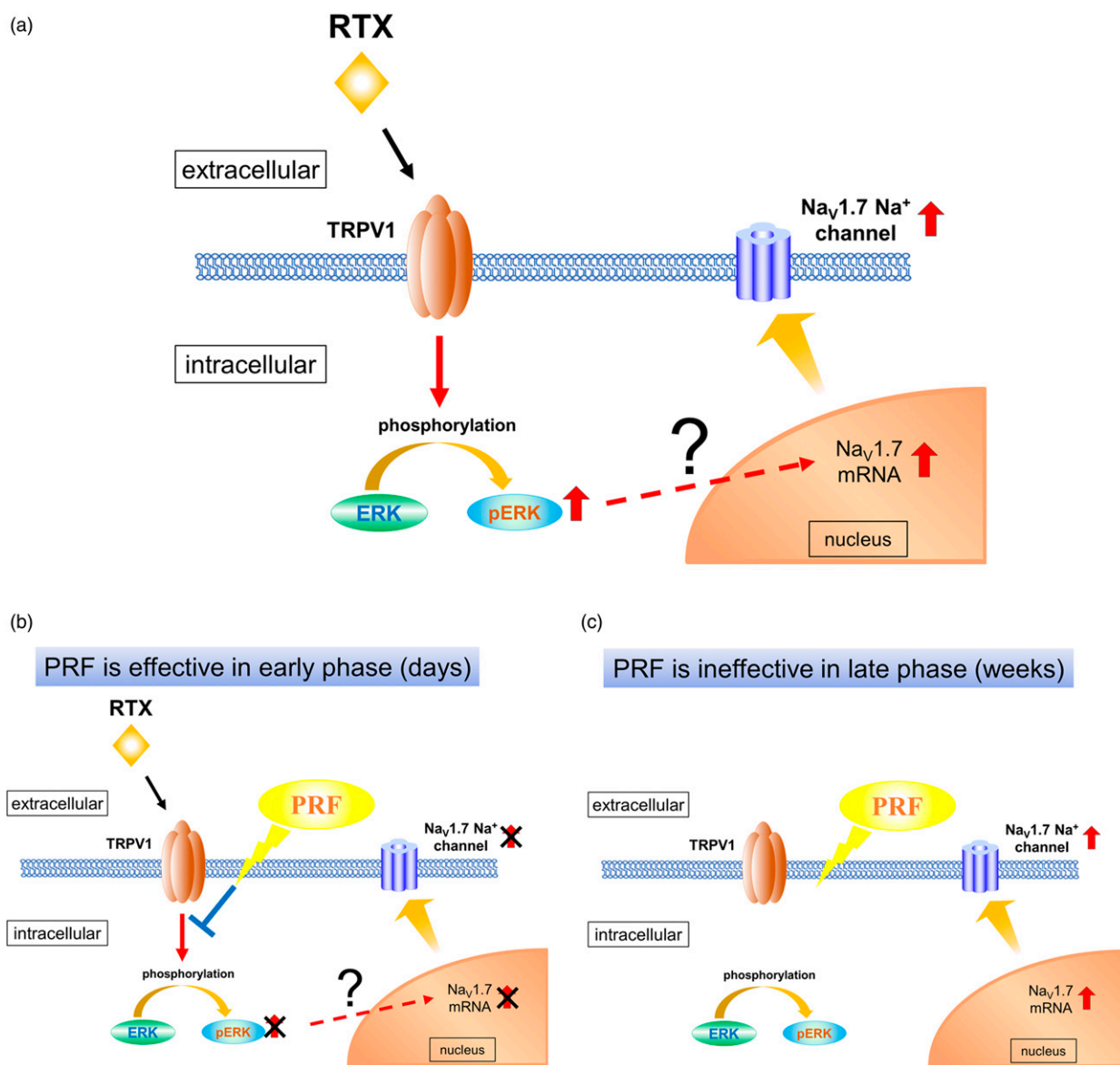


Figure 9. Development of RTX-induced neuropathic pain: a mechanism involving ERK and Na_v1.7 in DRG. (A) Schematic diagram of RTX-induced neuropathic pain pathophysiology. Binding of RTX to TRPV1 enhances ERK phosphorylation in DRG neurons, which may result in Na_v1.7 mRNA upregulation in the nucleus and Na_v1.7 expression upregulation. Enhanced ERK phosphorylation level returns to a steady state after RTX administration, whereas Na_v1.7 expression upregulation persists for several weeks, leading to a sustained painful condition. (B) In the early phase (days), PRF reduces pain by suppressing the RTX-induced enhancement of ERK phosphorylation and Na_v1.7 expression upregulation. (C) In the late phase (weeks), the enhanced ERK phosphorylation returns to a steady state level of phosphorylation. PRF therapy cannot suppress the RTX-induced pain, because it may not suppress Na_v1.7 expression upregulation. RTX, resiniferatoxin; PRF, pulsed radiofrequency; DRG, dorsal root ganglia; ERK, extracellular signal-regulated kinase; TRPV1, transient receptor potential vanilloid 1.

PRF application immediately after SNI surgery may be attributed to its inhibitory effect on ERK activation in dorsal horn cells. Lin et al.³⁷ showed that an early application of PRF adjacent to the DRG inhibited the activation of p38 and ERK in the dorsal horn and significantly reduced nerve ligation-induced mechanical allodynia and thermal hyperalgesia at

postoperative day 7 and days 3–7, respectively. Moreover, enhanced ERK phosphorylation has been shown to cause Na_v1.7 upregulation in some types of neuropathic pain.³² In this study, PRF therapy triggered RTX-induced mechanical allodynia recovery via early ERK phosphorylation attenuation and maintained this recovery by inhibiting Na_v1.7

upregulation after weeks (Figure 9). This may explain the differences in the mechanisms of PRF therapy in the early (days) and late (weeks) phases of neuropathic pain evolution.

In this study, delayed PRF therapy could not trigger RTX-induced mechanical allodynia recovery, which corroborated with the findings of Tanaka et al.¹⁰ PRF should be administered early in patients with PHN. Although the Japanese Committee for Clinical Practice Guideline for Chronic Pain strongly recommends PRF treatment for ZAP, especially PHN (grade 1A recommendation),³⁸ oral analgesics (tramadol and pregabalin) are often used in clinical practice prior to PRF therapy, which is often delayed. In this study, early tramadol treatment increased the efficacy of delayed PRF therapy in rats with RTX-induced mechanical allodynia. Na_v1.7 expression was suppressed in the DRG of rats in the RTX + tramadol + late PRF group, suggesting that RTX-induced allodynia is associated with an increase in Na_v1.7 expression, and suppressing Na_v1.7 upregulation will almost certainly lead to RTX-induced allodynia recovery. Therefore, it is appropriate to investigate why tramadol administration showed an analgesic effect even with delayed PRF treatment. Although our study did not prove the abovementioned mechanism, we coined the following hypothesis of the mechanism based on previous studies.

Neuropathic pain progresses from an “induction phase” (wherein symptoms gradually worsen) to a “maintenance phase” (wherein symptoms persist).³⁹ The activation of microglia and astrocytes in the spinal cord contributes to this phase change; the activation of microglia starts in the induction phase, and the activation of astrocytes coincides with both the transition and maintenance phases (Supplementary Figure 2).^{39,40} This phase change associated with a shift from microglial to astrocyte activation is also observed in RTX-induced neuropathic pain.¹² Furthermore, Sakakiyama et al.⁴¹ reported that tramadol exhibited preventive and alleviative (anti-allodynic) effects, via spinal astrocyte inhibition, in rats with neuropathic pain induced by partial sciatic nerve ligation. Thus, based on these findings and the present study results, we hypothesize that PRF becomes ineffective once RTX-induced neuropathic progresses to the “maintenance phase,” and tramadol delays the entry into the maintenance phase via astrocyte activity suppression; this might explain the restoration of the efficacy of delayed PRF treatment by tramadol.

This study had several limitations. First, we used RTX-treated rats as models for PHN. These PHN models had no connection with VZV infection. Therefore, our findings may not completely correspond to those obtained clinically. Second, although sex-related differences in pain thresholds may possibly exist, we did not focus on these differences in the current study; we customarily used male rats, as in many previous reports. Third, we did not directly demonstrate that an increase in ERK phosphorylation is associated with an upregulation of Na_v1.7 expression, using ERK inhibitors. Fourth, we focused on RTX-induced mechanical allodynia;

thermal allodynia was not investigated. Fifth, we did not investigate any mechanisms by which the use of tramadol restored the efficacy of delayed PRF treatment. Sixth, it would be important to know the duration of the effect of tramadol, by delaying the PRF treatment for an extended period; however, we did not investigate this duration. Hence, further investigations are required to compensate for the abovementioned limitations.

In conclusion, RTX-induced neuropathic pain is associated with ERK phosphorylation enhancement and Na_v1.7 expression upregulation in rat DRG. Early PRF therapy can trigger RTX-induced mechanical allodynia recovery, unlike delayed PRF therapy. By interposing early tramadol treatment, late PRF therapy can effectively trigger RTX-induced mechanical allodynia recovery. Our study findings may provide a better understanding of the molecular biological alterations involved in the development of PHN and help in designing effective therapeutic strategies.

Acknowledgments

The authors would like to thank Noriko Hidaka and Toshiko Watanabe for their technical and secretarial assistance in this study, and Editage (www.editage.com) for English language editing.

Author Contributions

KH, TM, and TK designed the experiments. KH, TM, MK, YK, and SK conducted the experiments and analyzed data. KH and TM drafted the manuscript. TS, RT, and IT supervised the experimental approach and corrected the manuscript. All authors have read and approved the final manuscript.

Declaration of Conflicting Interests

The author(s) declared no potential conflicts of interest with respect to the research, authorship, and/or publication of this article.

Funding

The authors disclosed receipt of the following financial support for the research, authorship, and/or publication of this article: This study was supported by a Grant-in-Aid for Scientific Research (KA-KENHI) [Grant Number: 18K16455]. Moreover, the study is attributed to the Department of Anesthesiology, Faculty of Medicine, University of Miyazaki.

ORCID iD

Toyoaki Maruta  <https://orcid.org/0000-0002-2660-2179>

Supplemental Material

Supplemental material for this article is available online.

References

1. Colloca L, Ludman T, Bouhassira D, Baron R, Dickenson AH, Yarnitsky D, Freeman R, Truini A, Attal N, Finnerup NB,

- Eccleston C, Kalso E, Bennett DL, Dworkin RH, Raja SN. Neuropathic pain. *Nat Rev Dis Primers* 2017; 3: 17002. DOI: [10.1038/nrdp.2017.2](https://doi.org/10.1038/nrdp.2017.2).
2. Choi EM, Chung MH, Jun JH, Chun EH, Jun IJ, Park JH, Choi E-H, Kim JE. Efficacy of intermittent epidural dexamethasone bolus for zoster-associated pain beyond the acute phase. *Int J Med Sci* 2020; 17: 1811–1818. DOI: [10.7150/ijms.46038](https://doi.org/10.7150/ijms.46038).
 3. Cohen JI. Clinical practice: herpes zoster. *N Engl J Med* 2013; 369: 255–263. DOI: [10.1056/NEJMcp1302674](https://doi.org/10.1056/NEJMcp1302674).
 4. Sumitani M, Sakai T, Matsuda Y, Abe H, Yamaguchi S, Hosokawa T, and Fukui S. Executive summary of the clinical guidelines of pharmacotherapy for neuropathic pain: second edition by the Japanese society of pain clinicians. *J Anesth* 2018; 32: 463–478. DOI: [10.1007/s00540-018-2501-0](https://doi.org/10.1007/s00540-018-2501-0).
 5. Boureau F, Legallicier P, Kabir-Ahmadi M. Tramadol in post-herpetic neuralgia: a randomized, double-blind, placebo-controlled trial. *Pain* 2003; 104: 323–331. DOI: [10.1016/s0304-3959\(03\)00020-4](https://doi.org/10.1016/s0304-3959(03)00020-4).
 6. Vuka I, Marciuš T, Došenović S, Ferhatović Hamzić L, Vučić K, Sapunar D, Puljak L. Efficacy and safety of pulsed radiofrequency as a method of dorsal root ganglia stimulation in patients with neuropathic pain: a systematic review. *Pain Med* 2020; 21: 3320–3343. DOI: [10.1093/pm/pnaa141](https://doi.org/10.1093/pm/pnaa141).
 7. Sluijter ME, Cosman E, Rittman W, Van Kleef M. The effect of pulsed radiofrequency fields applied to the dorsal root ganglion. *Pain Clin* 1998; 11: 109–117.
 8. Kim YH, Lee CJ, Lee SC, Huh J, Nahm FS, Kim HZ, Lee MK. Effect of pulsed radiofrequency for postherpetic neuralgia. *Acta Anaesthesiol Scand* 2008; 52: 1140–1143. DOI: [10.1111/j.1399-6576.2008.01752.x](https://doi.org/10.1111/j.1399-6576.2008.01752.x).
 9. Ding Y, Li H, Hong T, Zhao R, Yao P, Zhao G. Efficacy and safety of computed tomography-guided pulsed radiofrequency modulation of thoracic dorsal root ganglion on herpes zoster neuralgia. *Neuromodulation* 2019; 22: 108–114. DOI: [10.1111/ner.12858](https://doi.org/10.1111/ner.12858).
 10. Tanaka N, Yamaga M, Tateyama S, Uno T, Tsuneyoshi I, Takasaki M. The effect of pulsed radiofrequency current on mechanical allodynia induced with resiniferatoxin in rats. *Anesth Analg* 2010; 111: 784–790. DOI: [10.1213/ANE.0b013e3181e9f62f](https://doi.org/10.1213/ANE.0b013e3181e9f62f).
 11. Pan HL, Khan GM, Alloway KD, Chen SR. Resiniferatoxin induces paradoxical changes in thermal and mechanical sensitivities in rats: mechanism of action. *J Neurosci* 2003; 23: 2911–2919. DOI: [10.1523/JNEUROSCI.23-07-02911.2003](https://doi.org/10.1523/JNEUROSCI.23-07-02911.2003).
 12. Lei Y, Sun Y, Lu C, Ma Z, Gu X. Activated glia increased the level of proinflammatory cytokines in a resiniferatoxin-induced neuropathic pain rat model. *Reg Anesth Pain Med* 2016; 41: 744–749. DOI: [10.1097/AAP.0000000000000441](https://doi.org/10.1097/AAP.0000000000000441).
 13. Black JA, Frézel N, Dib-Hajj SD, Waxman SG. Expression of Nav1.7 in DRG neurons extends from peripheral terminals in the skin to central preterminal branches and terminals in the dorsal horn. *Mol Pain* 2012; 8: 82. DOI: [10.1186/1744-8069-8-82](https://doi.org/10.1186/1744-8069-8-82).
 14. Wada A. Roles of voltage-dependent sodium channels in neuronal development, pain, and neurodegeneration. *J Pharmacol Sci* 2006; 102: 253–268. DOI: [10.1254/jphs.crj06012x](https://doi.org/10.1254/jphs.crj06012x).
 15. Cummins TR, Howe JR, Waxman SG. Slow closed-state inactivation: a novel mechanism underlying ramp currents in cells expressing the hNE/PN1 sodium channel. *J Neurosci* 1998; 18: 9607–9619. DOI: [10.1523/JNEUROSCI.18-23-09607.1998](https://doi.org/10.1523/JNEUROSCI.18-23-09607.1998).
 16. Dib-Hajj SD, Yang Y, Black JA, Waxman SG. The Na(V)1.7 sodium channel: from molecule to man. *Nat Rev Neurosci* 2013; 14: 49–62. DOI: [10.1038/nrn3404](https://doi.org/10.1038/nrn3404).
 17. Liu C, Cao J, Ren X, Zang W. Nav1.7 protein and mRNA expression in the dorsal root ganglia of rats with chronic neuropathic pain. *Neural Regen Res* 2012; 7: 1540–1544. DOI: [10.3969/j.issn.1673-5374.2012.20.003](https://doi.org/10.3969/j.issn.1673-5374.2012.20.003).
 18. Kennedy PG, Montague P, Scott F, Grinfeld E, Ashrafi GH, Breuer J, Rowan EG. Varicella-zoster viruses associated with post-herpetic neuralgia induce sodium current density increases in the ND7-23 Nav-1.8 neuroblastoma cell line. *PLoS One* 2013; 8: e51570. DOI: [10.1371/journal.pone.0051570](https://doi.org/10.1371/journal.pone.0051570).
 19. Schneider CA, Rasband WS, Eliceiri KW. NIH Image to ImageJ: 25 years of image analysis. *Nat Methods* 2012; 9: 671–675. DOI: [10.1038/nmeth.2089](https://doi.org/10.1038/nmeth.2089).
 20. Xia Z, Xiao Y, Wu Y, Zhao B. Sodium channel Nav1.7 expression is upregulated in the dorsal root ganglia in a rat model of paclitaxel-induced peripheral neuropathy. *Springerplus* 2016; 5: 1738. DOI: [10.1186/s40064-016-3351-6](https://doi.org/10.1186/s40064-016-3351-6).
 21. Tamura R, Nemoto T, Maruta T, Onizuka S, Yanagita T, Wada A, Murakami M, Tsuneyoshi I. Up-regulation of Nav1.7 sodium channels expression by tumor necrosis factor- α in cultured bovine adrenal chromaffin cells and rat dorsal root ganglion neurons. *Anesth Analg* 2014; 118: 318–324. DOI: [10.1213/ANE.0000000000000085](https://doi.org/10.1213/ANE.0000000000000085).
 22. Obata K, Noguchi K. MAPK activation in nociceptive neurons and pain hypersensitivity. *Life Sci* 2004; 74: 2643–2653. DOI: [10.1016/j.lfs.2004.01.007](https://doi.org/10.1016/j.lfs.2004.01.007).
 23. Ji RR, Gereau RW 4th, Malcangio M, Strichartz GR. MAP kinase and pain. *Brain Res Rev* 2009; 60: 135–148. DOI: [10.1016/j.brainresrev.2008.12.011](https://doi.org/10.1016/j.brainresrev.2008.12.011).
 24. Yeh CC, Wu ZF, Chen JC, Wong CS, Huang CJ, Wang JS, Chien C-C. Association between extracellular signal-regulated kinase expression and the anti-allodynic effect in rats with spared nerve injury by applying immediate pulsed radiofrequency. *BMC Anesthesiol* 2015; 15: 92. DOI: [10.1186/s12871-015-0071-3](https://doi.org/10.1186/s12871-015-0071-3).
 25. Cai W, Zhao Q, Shao J, Zhang J, Li L, Ren X, Su S, Bai Q, Li M, Chen X, Wang J, Cao J, Zang W. MicroRNA-182 alleviates neuropathic pain by regulating Nav1.7 following spared nerve injury in rats. *Sci Rep* 2018; 8: 16750. DOI: [10.1038/s41598-018-34755-3](https://doi.org/10.1038/s41598-018-34755-3).
 26. Dai Z, Xu X, Chen Y, Lin C, Lin F, Liu R. Effects of high-voltage pulsed radiofrequency on the ultrastructure and Nav1.7 level of the dorsal root ganglion in rats with spared nerve injury. *Neuromodulation* 2021, DOI: [10.1111/ner.13527](https://doi.org/10.1111/ner.13527) (Accessed 13 April 2022), In preparation.
 27. Dai Y, Iwata K, Fukuoka T, Kondo E, Tokunaga A, Yamanaka H, Liu Y, Noguchi K. Phosphorylation of extracellular signal-regulated kinase in primary afferent neurons by noxious stimuli and its involvement in peripheral sensitization. *J Neurosci* 2002; 22: 7737–7745. DOI: [10.1523/JNEUROSCI.22-17-07737.2002](https://doi.org/10.1523/JNEUROSCI.22-17-07737.2002).

28. Zhuang ZY, Xu H, Clapham DE, Ji RR. Phosphatidylinositol 3-kinase activates ERK in primary sensory neurons and mediates inflammatory heat hyperalgesia through TRPV1 sensitization. *J Neurosci* 2004; 24: 8300–8309. DOI: [10.1523/JNEUROSCI.2893-04.2004](https://doi.org/10.1523/JNEUROSCI.2893-04.2004).
29. Maruta T, Nemoto T, Hidaka K, Koshida T, Shirasaka T, Yanagita T, Takeya R, Tsuneyoshi I. Upregulation of ERK phosphorylation in rat dorsal root ganglion neurons contributes to oxaliplatin-induced chronic neuropathic pain. *PLoS One* 2019; 14: e0225586. DOI: [10.1371/journal.pone.0225586](https://doi.org/10.1371/journal.pone.0225586).
30. Stamboulian S, Choi JS, Ahn HS, Chang YW, Tyrrell L, Black JA, Waxman SG, Dib-Hajj SD. ERK1/2 mitogen-activated protein kinase phosphorylates sodium channel Na(v)1.7 and alters its gating properties. *J Neurosci* 2010; 30: 1637–1647. DOI: [10.1523/JNEUROSCI.4872-09.2010](https://doi.org/10.1523/JNEUROSCI.4872-09.2010).
31. Nemoto T, Miyazaki S, Kanai T, Maruta T, Satoh S, Yoshikawa N, Yanagita T, Wada A. Na_v1.7-Ca²⁺ influx-induced increased phosphorylations of extracellular signal-regulated kinase (ERK) and p38 attenuate tau phosphorylation via glycogen synthase kinase-3beta: priming of Na_v1.7 gating by ERK and p38. *Eur J Pharmacol* 2010; 640: 20–28. DOI: [10.1016/j.ejphar.2010.04.048](https://doi.org/10.1016/j.ejphar.2010.04.048).
32. Wang GJ, Zhang X, Huang LD, Xiao Y. Involvement of the sodium channel Na_v1.7 in paclitaxel-induced peripheral neuropathy through ERK1/2 signaling in rats. *Curr Neurovasc Res* 2020; 17: 267–274. DOI: [10.2174/1567202617666200514113441](https://doi.org/10.2174/1567202617666200514113441).
33. Sun S, Sun J, Jiang W, Wang W, Ni L. Na_v1.7 via promotion of ERK in the trigeminal ganglion plays an important role in the induction of pulpitis inflammatory pain. *BioMed Res Int* 2019; 2019: 6973932. DOI: [10.1155/2019/6973932](https://doi.org/10.1155/2019/6973932).
34. Van Zundert J, de Louw AA, Joosten EJ, Kessels AH, Honig W, Dederen PWC, Veening JG, Vles JSH, van Kleef M. Pulsed and continuous radiofrequency current adjacent to the cervical dorsal root ganglion of the rat induces late cellular activity in the dorsal horn. *Anesthesiology* 2005; 102: 125–131. DOI: [10.1097/0000542-200501000-00021](https://doi.org/10.1097/0000542-200501000-00021).
35. Park HW, Ahn SH, Son JY, Kim SJ, Hwang SJ, Cho YW, Lee D-G. Pulsed radiofrequency application reduced mechanical hypersensitivity and microglial expression in neuropathic pain model. *Pain Med* 2012; 13: 1227–1234. DOI: [10.1111/j.1526-4637.2012.01453.x](https://doi.org/10.1111/j.1526-4637.2012.01453.x).
36. Hata J, Perret-Karimi D, DeSilva C, Leung D, Betesh N, Luo D, Dawodu S, Sinavsky K, Stokes OJ, English S. Pulsed radiofrequency current in the treatment of pain. *Crit Rev Phys Rehabil Med* 2011; 23: 213–240. DOI: [10.1615/CritRevPhysRehabilMed.v23.i1-4.150](https://doi.org/10.1615/CritRevPhysRehabilMed.v23.i1-4.150).
37. Lin ML, Lin WT, Huang RY, Chen TC, Huang SH, Chang CH, Tsai SY, Chiu HW, Yeh GC, Lin CW, Wen YR. Pulsed radiofrequency inhibited activation of spinal mitogen-activated protein kinases and ameliorated early neuropathic pain in rats. *Eur J Pain* 2014; 18: 659–670. DOI: [10.1002/j.1532-2149.2013.00419.x](https://doi.org/10.1002/j.1532-2149.2013.00419.x).
38. *The committee for clinical practice guideline for chronic pain.* https://plaza.umin.ac.jp/~jaspain/pdf/consortium_20180913en.pdf (Accessed 10 October 2021).
39. Shibata K, Sugawara T, Fujishita K, Shinozaki Y, Matsukawa T, Suzuki T, Koizumi S. The astrocyte-targeted therapy by Bushi for the neuropathic pain in mice. *PLoS One* 2011; 6: e23510. DOI: [10.1371/journal.pone.0023510](https://doi.org/10.1371/journal.pone.0023510).
40. Ji RR, Donnelly CR, Nedergaard M. Astrocytes in chronic pain and itch. *Nat Rev Neurosci* 2019; 20: 667–685. DOI: [10.1038/s41583-019-0218-1](https://doi.org/10.1038/s41583-019-0218-1).
41. Sakakiyama M, Maeda S, Isami K, Asakura K, So K, Shirakawa H, Nakagawa T, Kaneko S. Preventive and alleviative effect of tramadol on neuropathic pain in rats: roles of α -adrenoceptors and spinal astrocytes. *J Pharmacol Sci* 2014; 124: 244–257. DOI: [10.1254/jphs.13223fp](https://doi.org/10.1254/jphs.13223fp).